J Petrol Explor Prod Technol (2016) 6:729–742
DOI 10.1007/s13202-015-0214-6

ORIGINAL PAPER - PRODUCTION ENGINEERING

Condensate blockage effects in well test analysis of dual-porosity/dual-permeability, naturally fractured gas condensate reservoirs: a simulation approach

M. Safari-Beidokhti[1] · A. Hashemi[2]

Received: 21 June 2015 / Accepted: 29 October 2015 / Published online: 16 November 2015

Abstract Fluid flow in gas condensate reservoirs usually exhibit complex flow behavior when the flowing bottom-hole pressure drops below the dew-point. As a result, different flow regions with different characteristics are created within the reservoir. These flow regions can be identified by well test interpretation. The use of well test analysis for quantifying near well and reservoir behavior is well established for the case of simple single-layer homogenous systems. The behavior, however, is more complex in cases where different rock types or layering effects co-exist. In these cases, distinguishing between reservoir effects and fluid effects is challenging and needs a variety of analytical and numerical tools. The aim of this study is to investigate the liquid condensation effects on well test behavior of naturally fractured gas condensate through simulation approach in two different rock properties in a giant naturally fractured gas condensate field in south of Iran. A single well compositional model is developed to determine early-time, transition-time and late-time characteristics of the pressure transient data under condition of below dew-point pressure. Then compositional model has been used to verify the results obtained from conventional well test analysis in this field. The results of this study would improve modeling of the surrounding area in mentioned field. Interpretation of compositional model outputs have shown that condensate deposit near the wellbore yields a well test composite behavior in early and late time similar to what is found in single porosity homogenous system, but superimposed on double-permeability behavior. The behavior, however, is more complex in transition time which cause delay in hydrocarbon flow from the matrix blocks towards the fractures and lead to decrease in inter-layer cross flow coefficient.

Keywords Naturally fractured gas condensate reservoirs · Dual-porosity/dual-permeability model · Conventional well test analysis · Numerical simulation

Nomenclatures

c_t	Total compressibility (psi^{-1})
h_1, h_2	thickness of the layer (ft)
k_1, k_2	Permeability of the layer (mD)
k_m	Matrix permeability (mD)
k_f	Fracture permeability (mD)
k_{z1}, k_{z2}	Vertical permeability of the layer (mD)
k_{rg}	Gas relative permeability
P	Pressure (psi)
P_i	Initial pressure (psi)
r_w	Wellbore radius (ft)
ϕ	Porosity

Subscripts

f	Fracture
m	Matrix
i	Initial

Introduction

Gas condensate reservoirs

Condensate banking is formed as the pressure drops below dew-point which leads to reduce in well productivity in gas condensate reservoir. The gas relative permeability

✉ M. Safari-Beidokhti
mohsen.beidokhti@gmail.com

[1] Research Institute of Petroleum Industry (RIPI), Tehran, Iran

[2] Petroleum University of Technology (PUT), Abadan, Iran

decreases as the condensate saturation increases and thus the gas flow rate decreases by the time. The level of productivity decline depends on several factors, including critical condensate saturation, relative permeability, non-Darcy flow, and high capillary number effects (Bennion 2001; Whitson and Fevang 1999).

As many authors (Barnum et al. 1995; Boom et al. 1996) investigated, there are expected to have three different condensate saturation regions around the wellbore. The first region which is far away from the well, contains single gas phase include the initial liquid saturation, since the pressure is above the dew-point pressure. The second region which is near than to well commences with fall of pressure below dew-point pressure, and where the liquid saturation increases rapidly and consequently cause decreases in gas relative permeability considerably. The main note is the liquid in this intermediate region is immobile because the saturation of condensate still is lower than its critical value. Closer to the well and in the third region, the liquid saturation will exceed the critical saturation and then it is able to flow as gas. Many investigators have introduced the existence of the fourth region and effect of the capillary number through numerical studies (Gringarten et al. 2000), field production data (Boom et al. 1996) and laboratory experiments (Mott et al. 2000). So, the forth region which is formed in immediate vicinity of the wellbore creates considerable increase in well deliverability of the gas condensate reservoir. Figure 1 demonstrates the four different regions around the wellbore in the gas condensate reservoir.

The existence of aforementioned regions results in a three different mobility zones, exhibiting a three-region radial composite behavior (i.e., zones of different mobility and storativity) in well test analysis. Well test analysis is commonly used to identify and quantify near-wellbore effects, reservoir model and reservoir boundaries. Outcome all this information from well tests analysis in gas condensate reservoirs is challenging, because of changes in the composition of the original reservoir fluid and the impact of wellbore dynamics. Even so, gas condensate flow behavior is now well understood for simple single-layer homogenous reservoirs, in which the fluid flow toward the well can flow through one porous media. A number of publications (Daungkaew et al. 2002; Marhaendrajana et al. 1999; Saleh and Stewart 1992) have documented well tests in gas condensate single porosity homogenous reservoirs that exhibit regions of decreasing gas mobility near the wellbore and include an increased gas mobility region in the immediate vicinity of the wellbore (Gringarten et al. 2000; Daungkaew et al. 2002). Figure 2 illustrates the different regions (composite behaviors) around the wellbore in the single-porosity gas condensate reservoir using single-phase pseudo-pressure function.

However, the situation is different in gas condensate naturally fractured reservoirs. In this kind of reservoirs, these different regions are formed highly in the fracture networks due to high mobility of fractures and the gas saturation in matrix blocks does not change highly. Figure 3 depicts the gas saturation profile in naturally fracture reservoir (Ramirez et al. 2007).

Naturally fractured reservoirs

Naturally fractured reservoirs (NFR) has gained a large extend to the worldwide production of oil and gas which produce more than 50 % of world petroleum (Pápay 2003) and it is characterized a as a reservoir that contain fractures created by Mother Nature which can have either a positive or negative effect on fluid flow (Aguilera 1995).

Several reservoir idealizations have been introduced for modeling fluid flow in naturally fractured reservoirs. The dual-porosity idealization model was first introduced by Barenblatt (Barenblatt et al. 1960) which proposed a low

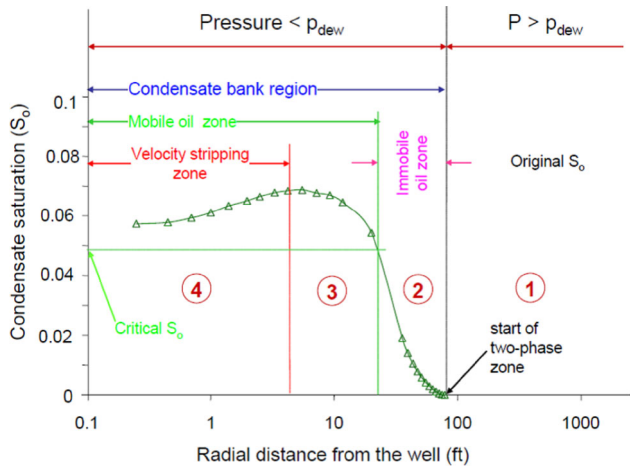

Fig. 1 Condensate saturation profile with condensate dropout and velocity stripping, (Gringarten et al. 2000)

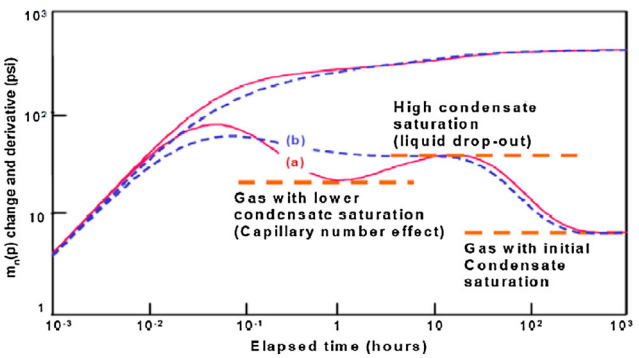

Fig. 2 Schematic of pressure and derivative of composite behaviors: (**a**) three and (**b**) two-region composite, (Gringarten et al. 2000)

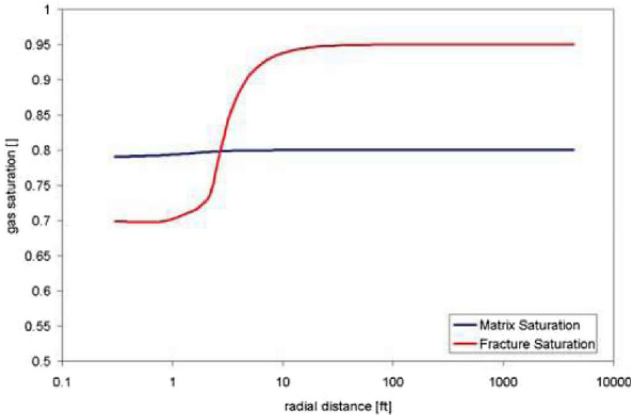

Fig. 3 Gas saturation profile for idealizations of dual-porosity/dual-permeability gas condensate reservoirs, (Ramirez et al. 2007)

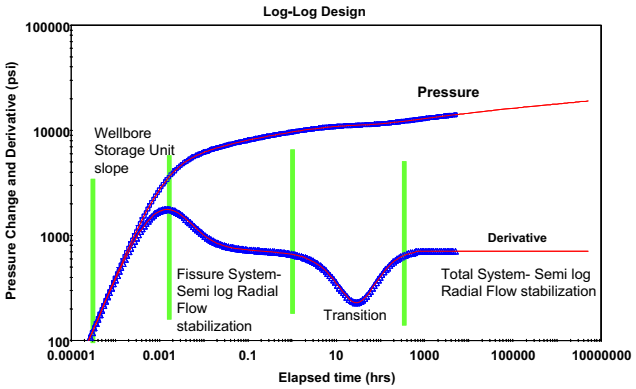

Fig. 4 Pressure and derivative log–log curve in dual-porosity reservoirs (Bourdet 2002)

permeability porous system, the matrix blocks, is surrounded by a fracture network of high permeability. This model was based on pseudo-steady state flow between the matrix blocks and the interconnected fractured system. The well test behavior of such reservoir is demonstrated in Fig. 4.

As an extension of the dual-porosity model which presented before, the dual-porosity/dual-permeability model is considered as a modified model in which flow to the wellbore occurs through both matrix and fracture systems. The dual-porosity/dual-permeability behavior is observed in stratified reservoirs, when the permeability of the different layers is participating to the response, or in fractured reservoirs, when the matrix blocks are connected (Bourdet 2002). Figures 5 and 6 represent a special dual-porosity and dual-porosity/dual-permeability model utilized by Ramirez (Ramirez et al. 2007) to simulate gas transient flow for well testing purposes. The model that was used to simulate gas condensate flow in the drainage area of a well is similar to this model.

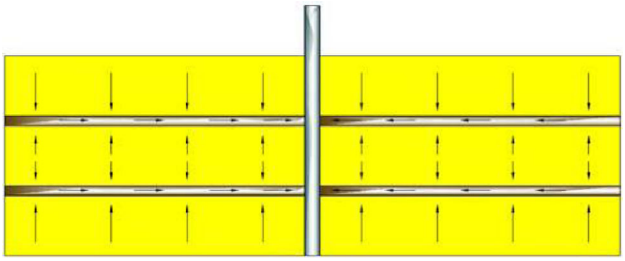

Fig. 5 Dual-porosity idealization of a naturally fractured reservoir, (Ramirez et al. 2007)

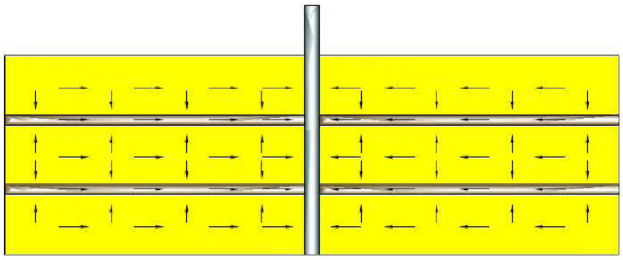

Fig. 6 Dual-porosity/dual-permeability idealization of a naturally fractured reservoir, (Ramirez et al. 2007)

As a general dual-porosity/dual permeability reservoir consists of two homogeneous layers which both layers can flow into the well, and there is flow between the layers in the reservoir. At any point in the reservoir the interlayer cross flow is proportional to the pressure difference between the two layers. The following parameters are used for description of this reservoir:

First one is mobility ratio, κ is defined as:

$$\kappa = \frac{k_1 h_1}{k_1 h_1 + k_2 h_2} = \frac{k_1 h_1}{k h_{\text{Total}}} \tag{1}$$

The second one is the storativity ratio, ω which is defined as:

$$\omega = \frac{(\phi C_t h)_1}{(\phi C_t h)_1 + (\phi C_t h)_2} = \frac{(\phi C_t h)_1}{(\phi C_t h)_{\text{Total}}} \tag{2}$$

The third one is interlayer cross flow coefficient, λ which is defined as:

$$\lambda = \frac{r_w^2}{k_1 h_1 + k_2 h_2} \cdot \frac{2}{\frac{h_1}{k_{z1}} + \frac{h_2}{k_{z2}}}. \tag{3}$$

When mobility ratio is equal to 1, the response is the same as the pseudo-steady state dual-porosity model because in pseudo-steady state dual-porosity model, only one porous medium is able to produce to the well, so $k_2 h_2$ is very low and negligible regarding to $k_1 h_1$. On the other hand, when mobility ratio decreases, the response tends to a homogeneous reservoir response, because in this situation, $k_1 h_1$ and $k_2 h_2$ tends to be the same value and mobility ratio reaches to value of 0.5 as illustrated in Fig. 7.

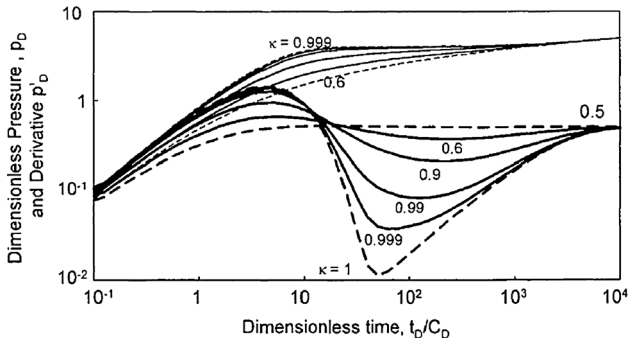

Fig. 7 Pressure and derivative log–log curve in dual-porosity/dual-permeability reservoir, the two dashed curves correspond to the homogenous reservoir responses ($\kappa = 0.5$) and dual-porosity response ($\kappa = 1$), (Bourdet 2002)

The performance naturally fractured gas condensate reservoirs would be more complicated regarding both rock and fluid effects. Consequently, distinguishing between reservoir effects and fluid effects is challenging in these specific reservoirs and needs numerical simulation. The present paper demonstrates how the flow regimes in dual-porosity/dual-permeability reservoir are affected by condensate accumulation and how this modifies the derivative shapes.

Approach

Since no analytical composite model has been published for naturally fractured gas condensate reservoirs in oil and gas literature, a numerical compositional simulator must be used to predict and analyze the corresponding well test behavior.

In this study, firstly conceptual compositional model is developed to investigate the condensate dropout effect on well test behavior of naturally fractured gas condensate reservoirs in two different scenarios. This knowledge is then applied to the analysis of actual field tests.

So, drawdown, build-up and multi-rate tests are conducted to establish the situation in which the flowing bottomhole pressure drops below the dew-point bringing about condensate forms. Both reservoir fluid and rock properties which are used in the compositional simulation are collected from a real naturally fractured gas condensate field in south of Iran. The results of the numerical model then were validated using standard well tests analysis to check the accuracy of model.

Secondly, we discuss the interpretation of well test data (DST) in a well A which is located in naturally gas condensate field in south of Iran by using modern well test techniques (Saphir software). Well test analysis of field data reveals that in the case of gas condensate naturally fractured reservoirs, the addition of condensate dropout increases the flow behavior complexity significantly.

At the end, compositional simulation was used to verify the results of analytical interpretations. Using the analytical well test interpretation results as inputs, the compositional model must provide an acceptable match on the pressure derivative, pressure history and condensate bank radius.

Conceptual numerical simulation studies

In this section, conceptual numerical model characteristic and development for dual-porosity/dual-permeability reservoirs containing two different rock properties presented and consequently the results are provided too.

Model set-up

A single vertical well model is set-up in radial coordinates with compositional simulator Eclipse-300 from Schlumberger. Radial coordinates are used to characterize a conceptual numerical multi-layer dual-porosity/dual-permeability reservoir of 140 ft thickness in two different rock properties in which a wide range of heterogeneities will be studied. In order to allocate perfect modeling near the wellbore gas condensate behavior, the number of grid block near the wellbore is too high and its size increases logarithmically away from the well (Fig. 8). The reservoir model grid data, production well information, initial reservoir saturation in both matrix and fracture are presented in Tables 1 and 2. The model does not account for

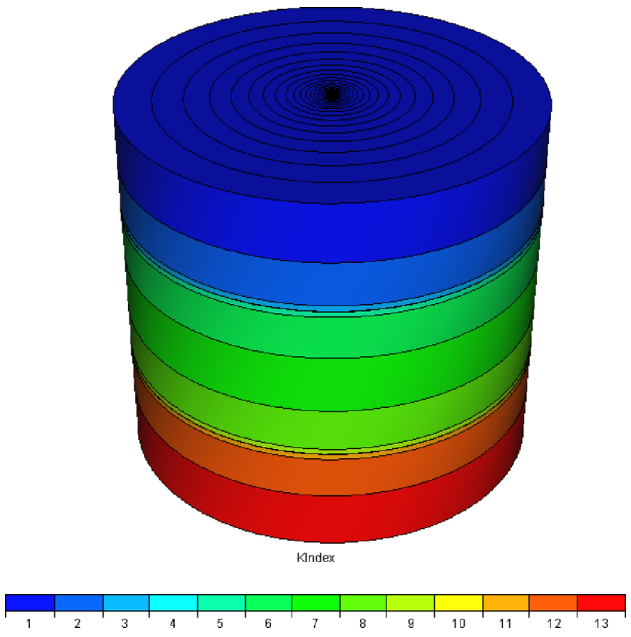

Fig. 8 Radial grid representation used in this study

Table 1 Reservoir simulation input data for conceptual numerical reservoir model

Grid information	
Number of cells in r-direction, I_{max}	45
Number of cells (layers) in z direction, K_{max}	13
Reservoir radius (r_e) (ft)	7000
Net to gross ratio	1
Thickness (ft)	140
Top depth (ft)	10,000
Well information	
Wellbore radius (r_w) (ft)	0.25
Wellbore storage coefficient (C_w) (RB/psi)	0
Roughness	0
Perforated nodes	1–13

Table 2 Initial saturation for conceptual numerical reservoir model

Initial saturation			
Matrix		Fracture	
S_{wi}	0.36	S_{wi}	0.05
S_{oi}	0.00	S_{oi}	0.00
S_{gi}	0.64	S_{gi}	0.95

wellbore storage or skin. Moreover, Frictional losses in the wellbore are also neglected.

Due to heterogeneity existence in naturally fractured gas condensate field in south of Iran, it has been tried to consider different rock properties in conceptual reservoir simulation models. Two simulation models with different rock properties [scenario 1 ($\kappa = 0.9$) and scenario 2 ($\kappa = 0.55$)] as shown in Table 3 were conducted and the results and analysis for condensate blockage effect on well test behavior of dual-porosity/dual-permeability naturally fractured gas condensate reservoirs are reported.

PVT modeling

To perform the reservoir simulation properly, the fluid properties need to be known over a wide range of temperatures and pressures. Hence, having perfect PVT matches [between equation of state (EOS) and experiments results] that play very important role in reservoir simulation analysis, are essential. So, here what is going to do is trying to find the best equation of state to get the best PVT matches. The PVTi package from Schlumberger is used to simulate the experiments. All experimental results are matched simultaneously to develop a representative EOS. A fluid sample is selected from a well A that reservoir pressure is greater than dew-point pressure so the fluid sample is gas. General PVT information is shown in the Table 4.

Finally, the 3-parameters Peng-Robinson (PR3) EOS is selected to generate the full range of PVT properties needed for input into the simulator in both scenarios. The original numbers of components without any Lumping are 51 components. But, the fluid components should be lumped into a smaller set of pseudo-components to decrease CPU and time demands. Subsequently, EOS matching with 8 components provided good agreement for the dew-point pressure and maximum liquid dropout in the Constant volume depletion (CVD) experiment. The final numbers of components, grouping components and their mole fractions is illustrated in Table 5. Also, Table 6 summarizes the detail results of PVT matching. In addition, Figs. 9 and 10 show Comparison between calculated and observed constant composition expansion (CCE) and CVD experiment, Liquid saturation, respectively.

Relative permeability

Since in naturally fractured reservoirs two different porous media exist in the reservoir, two relative permeability

Table 4 General PVT information

Well	A
Reservoir fluid	Gas condensate
Current reservoir pressure	5230 psia
Reservoir temperature	212 °F
CGR	42 STB/MMSCF

Table 3 Rock properties for conceptual numerical reservoir model (scenario 1 and 2)

Rock properties							
Scenario 1 ($\kappa = 0.9$)				Scenario 2 ($\kappa = 0.55$)			
Matrix		Fracture		Matrix		Fracture	
k (md)	3	k (md)	10,000	k (md)	5	k (md)	1000
h (ft)	139.2	h (ft)	0.4	h (ft)	138.3	h (ft)	0.85
ϕ	0.11	ϕ	1	ϕ	0.11	ϕ	1
C_f (psi^{-1})	4.25E−06	C_f (psi^{-1})	1E−4	C_f (psi^{-1})	4.25E−06	C_f (psi^{-1})	1E−4

Table 5 Final composition of gas condensate fluid

Number	Components	Mole fraction
1	PC1 (C1, N2)	86.03
2	C2	5.24
3	PC2 (C3, H2S)	2.19
4	CO2	1.93
5	PC3 (iC4, nC4, C5, iC5, nC5)	1.75
6	PC4 (C6, BEN, C7, TOL, C8, C9, C10, C11, C12)	2.34
7	PC5 (C13 to C19)	0.42
8	PC6 (C20 to C35 and C36+)	0.1

curves should be defined for each medium. Matrix relative permeability characteristics based on information taken from core analysis in lab was fed into the simulator. Since matrix relative permeability highly depends on velocity and IFT in gas condensate reservoirs, Eclipse-300 interpolates the gas relative permeability curve between a base and a miscible fluid relative permeability curve. The matrix relative permeability curve is shown in Fig. 11. Furthermore, Fig. 12 shows fracture relative permeability curve is considered as straight line because of its high mobility.

Model validation

The simulated flowing bottom-hole pressures of scenario 2 are considered as a real case and are analyzed using standard well test analysis package in order to verify the accuracy of the numerical model. For this purpose, build-up analysis is carried out to investigate differences between the real field data (input data of simulator) and simulation results. Comparison between input data of the simulation model and results of build-up analysis above the dew-point pressure shows good matches that are presented in Table 7.

Simulation results

The simulation runs were designed to generate the derivative shapes that could be expected in dual-porosity/dual-permeability well responses tests in gas condensate reservoirs below the dew-point pressure under various conditions. In all cases, the initial reservoir pressure was set just above the dew-point pressure so that a liquid-phase condensate forms at the start of production. The models were run for a total of 178 days and were assumed to produce at different rates which are shown in the Table 8. An example of pressure-rate history for a simulation run in the scenario 1 and 2 are shown in Figs. 13 and 14, respectively.

Table 6 Comparison between observed and calculated PVT data

Observed dew point pressure (psia)	Calculated dew point pressure (psia)	Maximum liquid dropout in the CVD experiment (% difference between observed and calculated)	Maximum liquid dropout in the CCE experiment (% difference between observed and calculated)
4898	4891.4	4	6

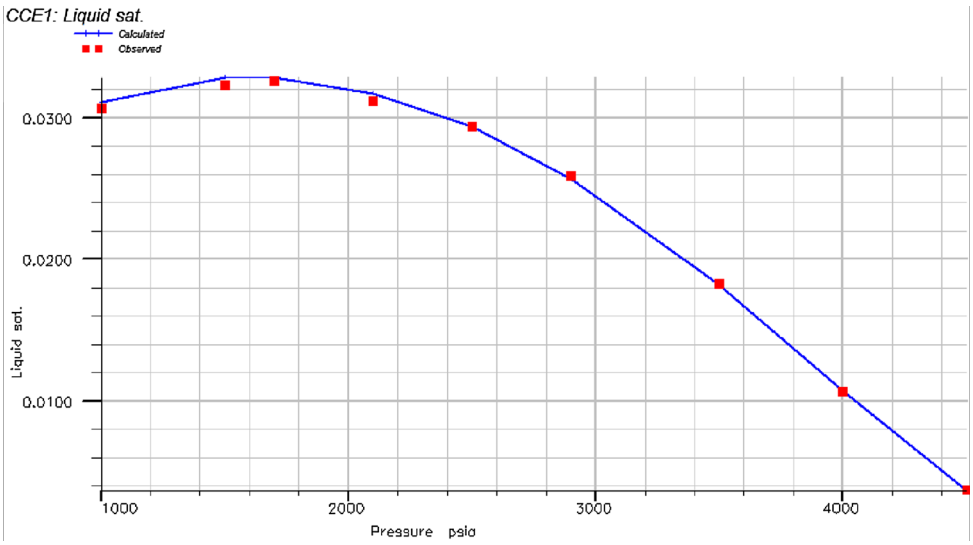

Fig. 9 Comparison between calculated and observed CCE experiment, liquid saturation

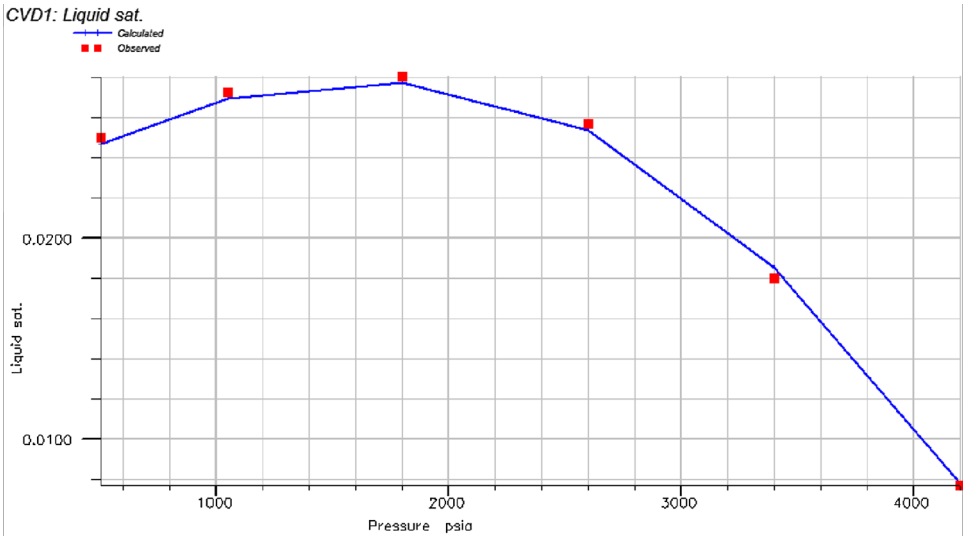

Fig. 10 Comparison between calculated and observed CVD experiment, liquid saturation

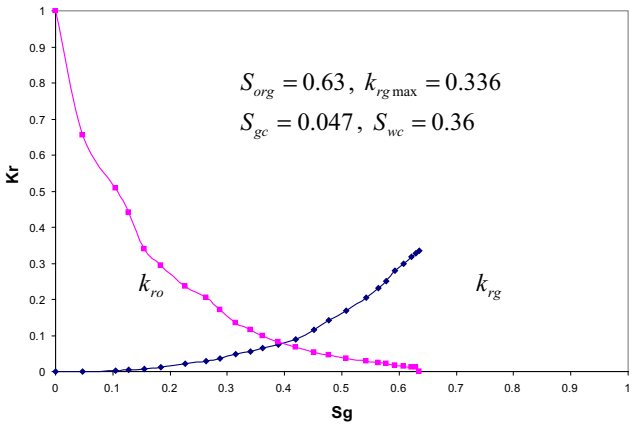

Fig. 11 Gas/oil relative permeability curves in the matrix used in the simulation

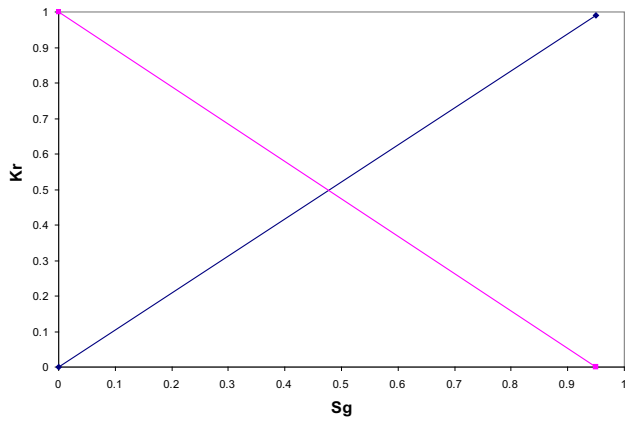

Fig. 12 Gas/oil relative permeability curves in the fracture used in the simulation

Table 7 Build-up test analysis for reservoir model above the dew-point pressure

	Simulation input data	Log-log analysis of simulation results
P_i (psia)	6000	5984
kh (md − ft)	480	452
k_{reff} (md)	4.61	4.34

Table 8 Rate schedule for conceptual simulation run

Elapse time (h)	Gas rate (Mscf/day)
9.6	6000
9.6	0
600	8000
9.6	0
1200	10,000
9.6	0
2400	12,000
25	0

As can be seen in both Figs. 13 and 14, the total test consists of eight periods of alternating drawdowns and buildups, labeled DD1, BU1, DD2, BU2, etc. Because the pressure drawdown is small in naturally fractured reservoirs, the gas flow rates and the durations of the drawdown periods (except DD1) were selected large enough so that condensate could accumulate and be detected on the derivative during the different dual-porosity/dual-permeability flow regimes. The first drawdown was at very low flow rate (6000 Mscf/D) and of short duration (9.6 h) to

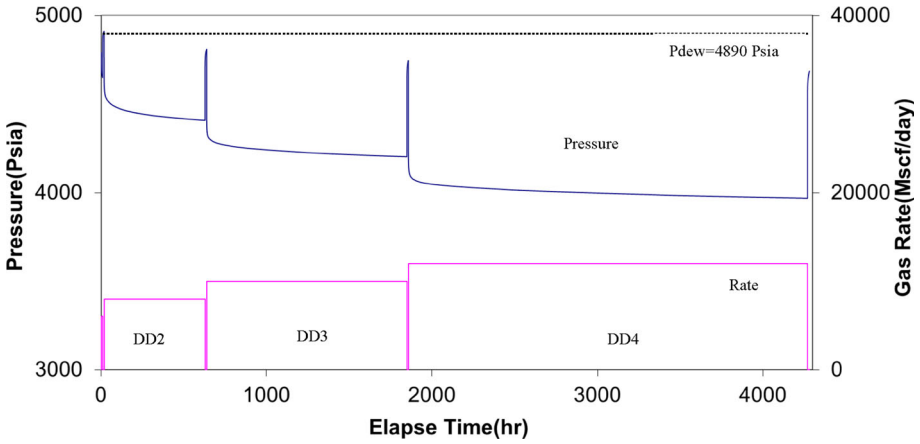

Fig. 13 Pressure-rate history example for the simulation run, scenario 1

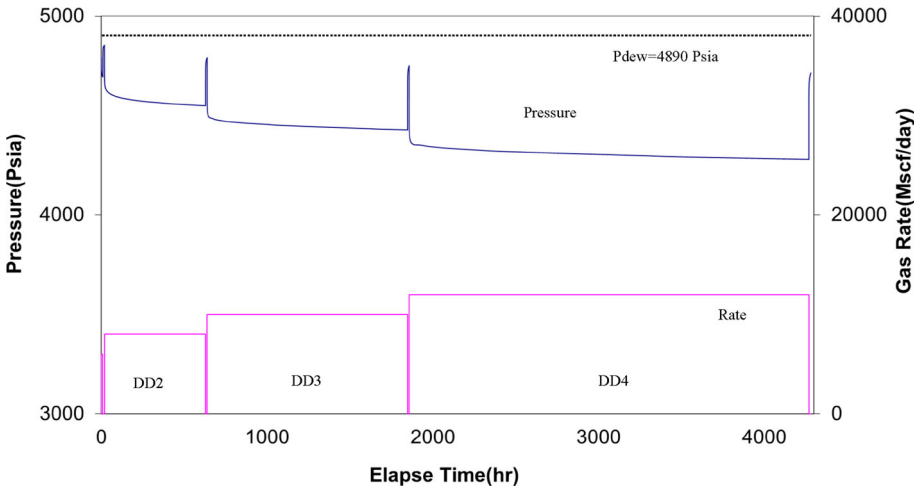

Fig. 14 Pressure-rate history example for the simulation run, scenario 2

demonstrate a dual-porosity/dual-permeability well test behavior near the dew-point pressure for comparison.

Discussion

Different flow behaviors that can be observed on a producing well response in dual-porosity/dual-permeability reservoir are discussed in both scenarios as follows:

Scenario 1 As it was shown in Fig. 13, all the drawdown and buildup flow periods (except BU1) are below the dew-point pressure. Consequently, a condensate bank is expected to be developed in the fracture systems. This is verified in Fig. 15, where the condensate saturation is plotted vs. radial distance at different production times.

Figure 16 shows a diagnostic log–log plot of single pseudo-pressures and derivatives for the different flow. Different flow behaviors in this figure which can be observed on a producing well response in dual-porosity/dual-permeability reservoir are discussed in three different categories such as early times, transition times and late times behaviors:

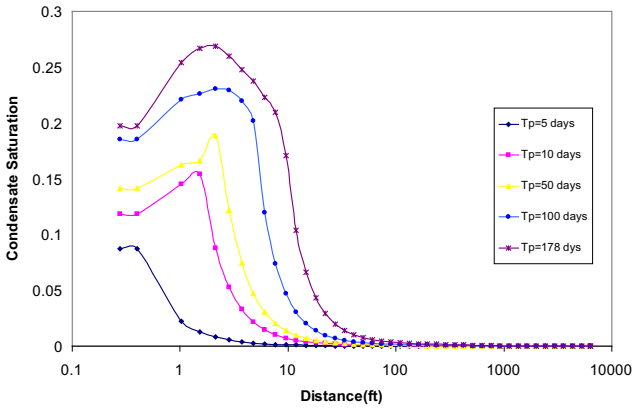

Fig. 15 Condensate distribution in the reservoir over the entire rate history of scenario 1 (model with N_c)

1. Early times behavior

A composite behavior due to condensate banking is superimposed on dual-porosity/dual-permeability flow behavior (BU1) in early times. From the derivative shapes (Fig. 16), it is clear that when bottomhole pressure falls

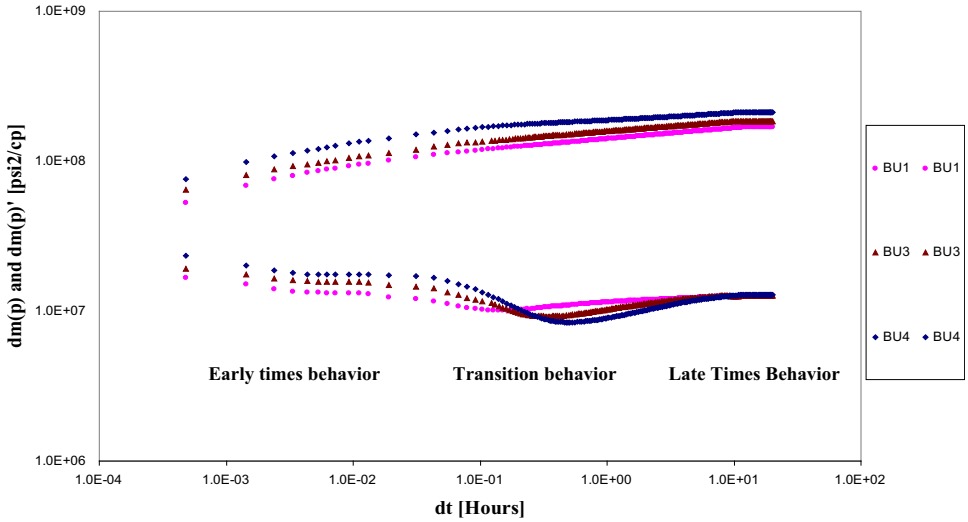

Fig. 16 Log–log diagnostic of the main flow periods considered in scenario 1

below the dew-point, a near-wellbore zone with a reduced mobility is created. This behavior is first characterized by an upward shift of the early times derivative stabilization as in BU3. As production time increases, more condensate is accumulated, and that is why BU4 has a lower mobility zone compare to the previous build-up (BU3). As a result, the effect of the condensate blockage on early times is the same as in the case of the composite homogenous flow behavior.

2. Transition times behavior

Since at transition regime fluid transfer between the layers (matrix and fractures) starts in the reservoir, any restriction which causes limitation of the layers communication results in increasing the duration of this period. Interpretations of log–log analysis (Fig. 16) have revealed that the liquid condensation causes damage of the surface of the matrix blocks due to introduced interporosity skin factor. This amount of skin factor causes delaying matrix feeding to fractures and result in decreasing of interlayer cross flow coefficient, λ. This fact brings about pressure derivative curve shifts to the right and becomes deeper in transition period. As production time increases, more liquid condensation forms which means more restriction for supplying the fractured network by matrix blocks. Therefore, the diagnostic gas condensate in double-permeability reservoir characteristics of pressure derivative below the dew-point shifts more to the right and in the shape of a trough becomes more pronounced in transition time. As a result, because higher condensate saturation due to more production time is formed (BU4), the amount of the skin factor is higher and consequently result in more decrease in interlayer cross flow coefficient, λ which is shown in Table 9.

3. Late times behavior

Since average reservoir pressure is greater than the dew-point in region which is located far away from the wellbore, no liquid formed in that region. Therefore, late-times stabilization is the same in all cases (BU1, BU3 and BU4). This fact is also obvious in which the derivative stabilization after 10 h of shutting well (Build-up) are the same for all cases.

Table 9 Interlayer cross flow coefficient (λ) in different build-up flow periods (scenario 1)

Build-up flow period	Interlayer cross flow coefficient (λ)
BU1 (no liquid condensation)	4.8E−5
BU3	3.49E−5
BU4	1.95E−5

Scenario 2 As it was illustrated in the Fig. 14, all the drawdown and buildup flow periods (except BU1) are below the dew-point pressure. Therefore, a condensate bank is expected to be developed in the fracture network. This is verified in Fig. 17, where the condensate saturation is plotted vs. radial distance at different production times. Figure 18 depicts a diagnostic log–log plot of single pseudo-pressures and derivatives for the different flow periods. As it is shown in this figure, a composite behavior due to condensate banking (BU3 and BU4) is superimposed on the dual-porosity/dual-permeability behavior (BU1). Noted, since the difference between permeability thickness (kh) of the matrix and fracture ($\kappa = 0.55$) is low, no transition period (no humping) can be observed in log–log derivative plot. Moreover, it is clear that when the flowing bottomhole pressure drops below the dew-point, a near-wellbore zone with a reduced mobility is created. This behavior is first characterized by an upward shift of the early time derivative stabilization, as in BU3. As production time increases, more condensate is formed which results in more upward shift of early time (BU4).

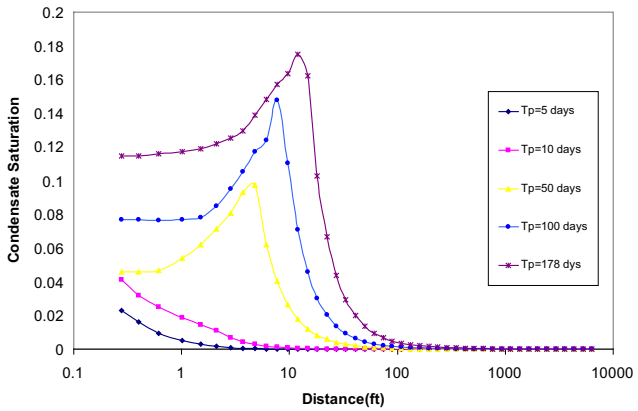

Fig. 17 Condensate distribution in the reservoir over the entire rate history of scenario 2 (model with N_c)

Furthermore, because the average pressure of the reservoir is still above the dew-point, liquid condensation dose not form in entire reservoir ($R_{i,\max} = 180$ ft). Thus late-times stabilization is the same in all cases (BU1, BU3 and BU4).

Also, Fig. 18 shows an increase in the skin factor as producing time increases. This is indicated by the different levels of the pressure curves. Because we did not take into account the mechanical skin in the simulation, and because the gas flow rate increases all consecutive flow periods, this increase in skin is due to the non-Darcy flow and condensate drop as well. Additionally, the decreasing trend in condensate distribution in vicinity of the well (Fig. 17) shows the effect of the N_c that compensate the non-Darcy effects. The simulation study thus confirms that condensate deposit near the wellbore yields a well test composite behavior and an increase in the value of the skin factor. So, as a result the composite behavior in dual-porosity/dual-permeability reservoirs in which low difference between permeability thickness (kh) of the matrix and fracture ($\kappa = 0.55$) exist is similar to that of in composite single-porosity homogenous reservoirs.

Analytical well test analysis of well A

Well A is a vertical well, completed with a perforations liner. The perforation interval covers 140 ft of K2 in the interval between 9046 and 9186 ft TVD. The producing interval was tested in one stage and DST was performed in March 1999. The pressure-rate history of the DST is shown in Fig. 19. The entire DST was divided into 19 separate flow periods, each one corresponding to a constant rate. The flowing bottomhole pressure was below the dew-point during the drawdown periods, but the down-hole shut-in pressure was above the dew-point in the main shut-in periods (BU19). The results of well test analysis and the best model matches (two layers reservoir model) provided in the Figs. 20 and 21.

Since no composite model exists for dual-porosity/dual-permeability reservoir, the condensate bank in well A cannot be treated explicitly, as in the case of simple single-layer homogenous reservoirs. So, the matches were poor and needed for compositional simulation become important.

Compositional simulation of well test in well A

In this section, numerical compositional model is used to simulate the entire production history in DST test of well A. Contrary to conventional well test analysis; compositional simulations take into account the changes in the composition of the initial gas/condensate fluid over the entire production period. This approach thus can validate results obtained from conventional well test analysis and provide detailed information on the different near-wellbore effects caused by condensate dropout.

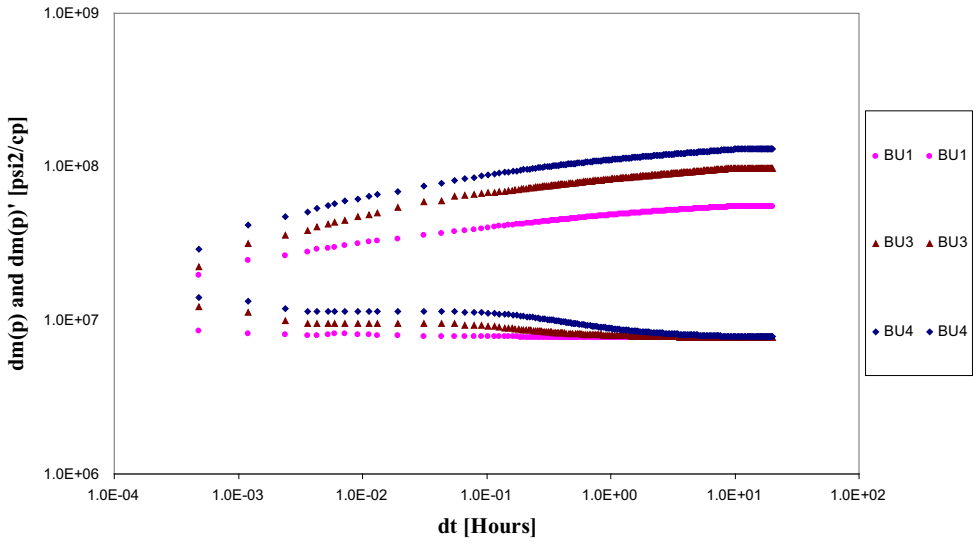

Fig. 18 Log-log diagnostic of the main flow periods considered in scenario 2

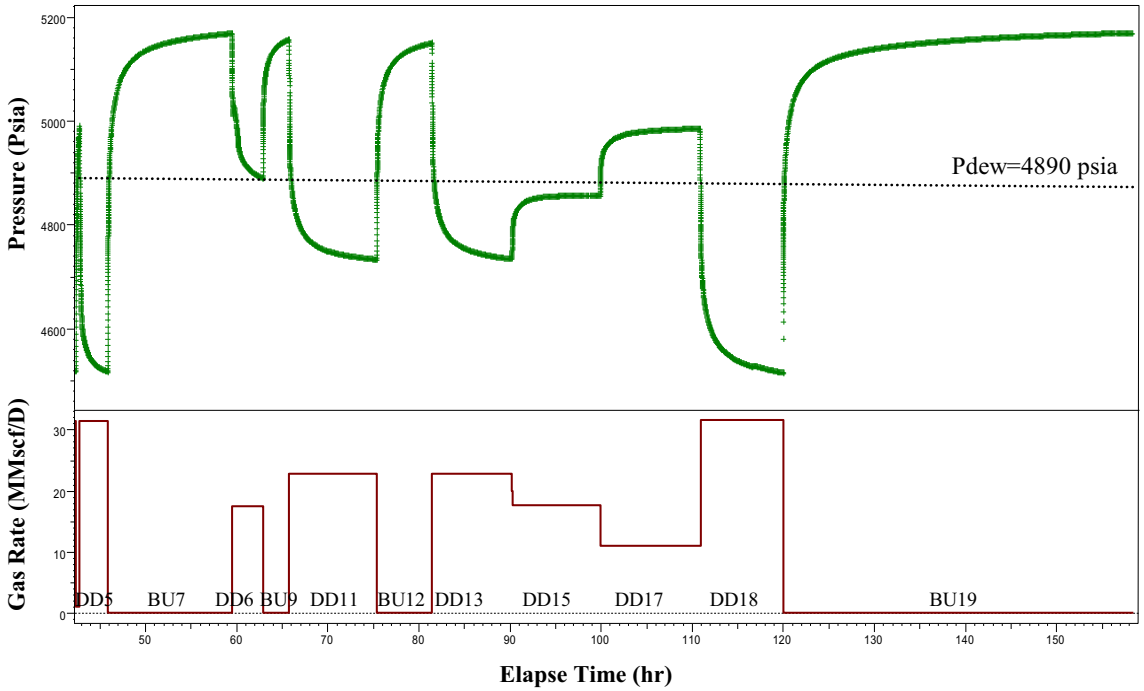

Fig. 19 Pressure/rate history of the DST, well A

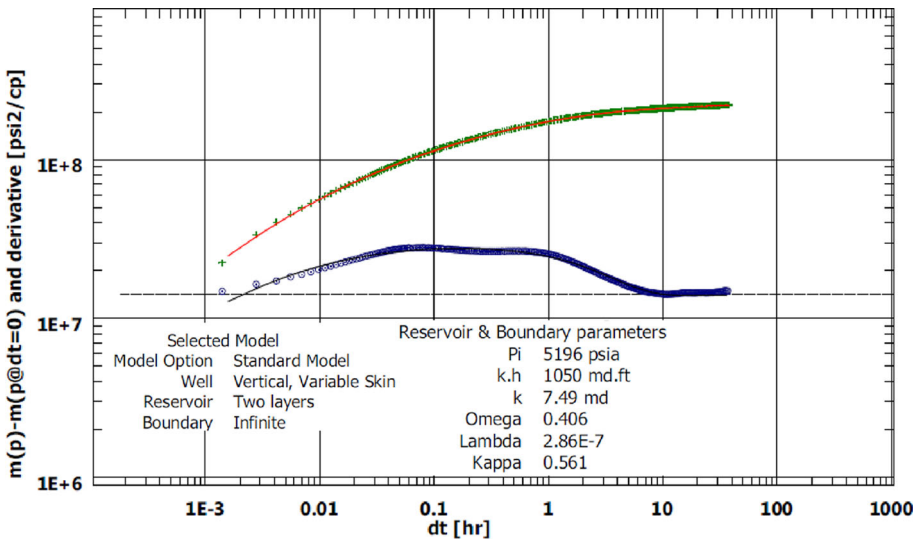

Fig. 20 Log-log match, BU19, well A

A single well compositional model with the same grid blocks configuration as conceptual numerical model was used for the compositional simulation. Production well information, initial reservoir saturation in both matrix and fracture, PVT characteristics of the reservoir fluid and also the relative permeability characteristics are equal to those ones used in the conceptual numerical model. It should be mentioned that the non-Darcy coefficient was determined from experiment and also basic reservoir parameters was determined from well test analysis. Wellbore storage and frictional losses in the wellbore were not simulated. The reservoir depth and gas/water contact (GWC) were obtained from the field history report.

Since the matrix and fracture permeability are unknown, sensitivity runs were made on matrix and fractured permeability in order to get an acceptable match between simulation bottomhole pressure and field flowing bottom-hole pressure. The model was initially run to ensure that the simulation response matched the entire pressure history of DST test. Because the main drawdown flow periods (DD5, DD11, DD13 and DD18) are conducted slightly below the dew-point and for very short times, pressure drawdowns are

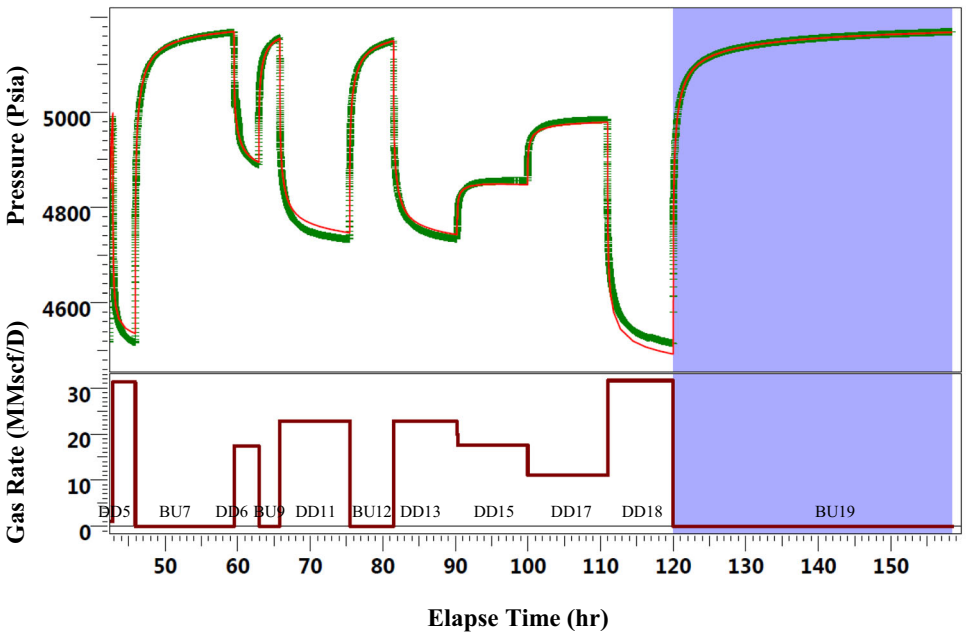

Fig. 21 Pressure/rate history match, BU19, well A

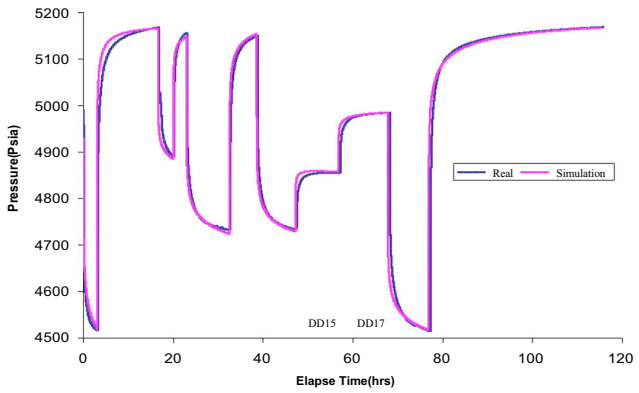

Fig. 22 Pressure history match of well A

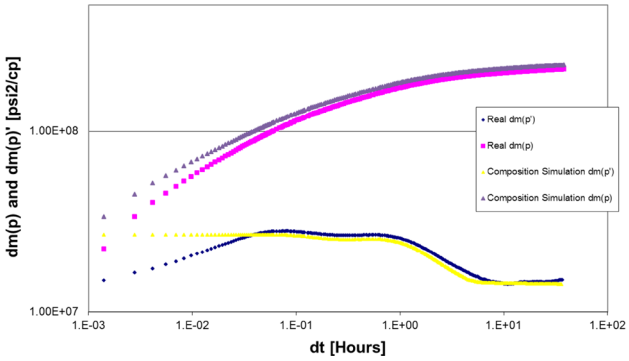

Fig. 23 Log-log match of compositional model responses (BU19)

governed by non-Darcy flow and mechanical skin only. A mechanical skin of -1.5 in the simulation model provided a reasonable match on the DST. This value was kept constant on all simulations to see whether it matched the corresponding drawdown flow periods in the production tests. The reasonable DST match shown as a red line in Fig. 22 suggests that the total permeability, condensate bank radius and the initial reservoir pressure estimated from conventional well test analysis are reasonably accurate. Moreover A log–log plot of single-phase pseudo-pressures and derivatives for the flow period BU19 (Fig. 23) shows that almost the simulated case matches the corresponding actual derivatives at transient and late times. As expected, the matches are not as good at early times because the compositional model does not account for wellbore storage effects.

Figure 24 also shows the condensate distribution in the reservoir (fracture system) at the end of the DST test (BU19) which could not be obtained from conventional analysis. During the DST (BU19), the pressure drawdown is low, and the condensate bank radius is less than 100 ft. The condensate saturation is less than the critical condensate saturation, even very near the wellbore and the effect of the capillary number cannot be detected. As a result, only two regions can be identified: (1) region in which only the gas phase is flowing and the oil phase is present but is immobile, and where oil saturation increases dramatically; and (2) an outer region, in which only the gas phase is present. In addition, Table 10 shows the differences between simulation outcomes and analytical well test analysis. However, in some flow periods (DD15 and DD17) the matches are worse because the model overestimated the bottomhole pressure. These differences most likely result from differences in the PVT used by the simulator and well tests software (Saphir software). Moreover, the matches in early times of the all flow periods

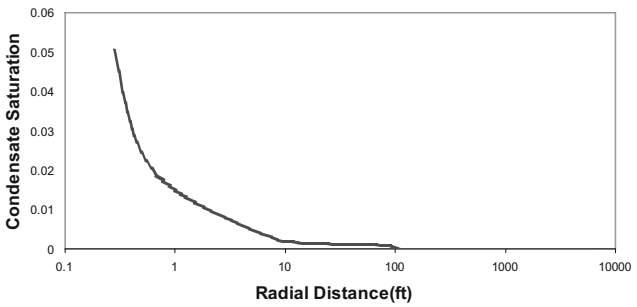

Fig. 24 Condensate distribution in well A at the end of DST test (BU19)

Table 10 Comparison between well test and simulation results in well A

	Well test results	Simulation results	Unit
kh	1050	1071	md ft
P_i	5196	5200	psia
k_m	–	2	md
k_f	–	8000	md
Skin	−3	−1.5	–
R_i	–	109	ft

are poor because the simulation model cannot simulate the wellbore storage in the well.

Conclusion

The outcomes of this dual-porosity/dual-permeability reservoir simulator for naturally fractured gas condensate reservoirs which associated by condensate deposition lead to following conclusion:

1. Actual well test behaviors were consistent with the behaviors predicted from compositional simulations (scenario 2).
2. Using analytical conventional interpretation techniques in well test analysis of dual-porosity/dual-permeability naturally fractured gas condensate reservoirs which suffer condensate blockage issues leads to misinterpretation results. This problem implies applying numerical studies to gain more accurate results.
3. According to the conceptual numerical composition results:
   - In both scenarios as production time goes by, the amount of condensate saturation near the wellbore increases that lead to increase total Skin factor.
   - In the case of high difference between permeability thickness (kh) of the fracture and matrix (scenario 1), according to the pressure derivative curve, a composite behavior due to condensate banking is superimposed on dual-porosity/dual-permeability flow behavior in early times but the transition times is shifted to the right and down because of decreasing interlayer cross flow coefficient due to interporosity skin factor that is formed by condensation banking.
   - In the case of the low difference between permeability thickness (kh) of the fracture and matrix (scenario 2), it is found that the condensate deposition creates a composite well test behavior similar to what is obtained in single-porosity reservoirs, but superimposed on a dual-porosity/dual-permeability flow behavior.
4. Based on two cases (scenario 1 and 2), although the enhanced permeability region due to N_c effects is not obvious in the log–log diagnostic plots but probably does exist. This is supported by the plot of condensate distribution within the reservoir that shows the decreasing trend in the vicinity of the well. Thus suggesting that non-Darcy effects are being compensated for by N_c effects.

Acknowledgments The authors would like to thank POGC for their support and permission to publish this work.

References

Aguilera R (1995) Naturally fractured reservoirs. PennWell Publishing Company, Tulsa. ISBN 0-87814-449-8

Barenblatt GJ, Zheltov IP, Kochine IN (1960) Basic concept of the single phase flow through fractured porous media. Prikladnaia Maternatika i Mechanika, Academia Nauk, S.S.S.R 24(5):852–864

Barnum RS, Birkman FP, Richardson TW, Spillette AG (1995) Gas condensate reservoir behavior: productivity and recovery reduction due to condensation. In: SPE 30767 presented at the SPE annual technical conference and exhibition, Dallas, Texas, October

Bennion DB (2001) Improving well productivity by evaluating and reducing formation damage during overbalanced and underbalanced drilling operations. PhD Thesis, University of Calgary, April

Boom W, Wit K, Weeda HC, Maas JG (1996) On the use of model experiments for assessing improved gas-condensate mobility under near- well bore flow conditions. In: SPE 36714, prepared for presentation at the SPE annual technical conference and exhibition, Denver, Colorado, October, pp 343–353

Bourdet D (2002) Well test analysis: the use of advanced interpretation model. Elsevier Scientific Publishing Co., Paris

Daungkaew S, Ross F, Gringarten AC (2002) Well test analysis of condensate drop-out behavior in a north sea len gas condensate reservoir. In: SPE 77548 presented at the SPE annual technical conference and exhibition, San Antonio, Texas, 29 September, 2 October

Gringarten AC, Al-Lamki A, Daungkaew S (2000) Well test analysis in gas condensate reservoirs. In: SPE 62920 presented at the SPE annual technical conference and exhibition, Dallas, Texas, October

Marhaendrajana T, Kaczorowski NJ, Blasingame TA (1999) Analysis and interpretation of well test performance at Arun Field, Indonesia. In: SPE 56487 presented at the SPE annual technical conference and exhibition, Houston, 3–6 October

Mott R, Cable A, Spearing M (2000) Measurements and simulation of inertial and high capillary number flow phenomena in gas-condensate relative permeability. SPE 62932 presented at the SPE Annual Technical Conference and Exhibition, Dallas, Texas, October

Pápay J (2003) Development of petroleum reservoirs. Akadémiai Kiadó Publishers, Budapest. ISBN 963-05-7917-8

Ramirez B, Kazemi H, Ozkan E (2007) Non-darcy flow effects in dual-porosity, dual-permeability, naturally fractured gas condensate reservoirs. In: SPE 109295 presented at the SPE annual technical conference and exhibition held in Anaheim, California, USA, 11–14 November

Saleh AM, Stewart G (1992) Interpretation of gas condensate well tests with field examples. In: SPE 24719 presented at the SPE annual technical conference and exhibition, Washington, DC, 4–7 October

Whitson CH, Fevang O (1999) Gas condensate relative permeability for well calculation. In: SPE 56476 presented at the SPE annual technical conference and exhibition, Houston, Texas, October